Property change in ZrN_xO_y thin films: effect of the oxygen fraction and bias voltage

F. Vaz[a,*], P. Carvalho[a], L. Cunha[a], L. Rebouta[a], C. Moura[a], E. Alves[b],
A.R. Ramos[b], A. Cavaleiro[c], Ph. Goudeau[d], J.P. Rivière[d]

[a]Departamento Física, Universidade do Minho, Campus de Azurém, 4800-058 Guimarães, Portugal
[b]Departamento de Física, ITN, E.N. 10, 2686-953 Sacavém, Portugal
[c]ICMES, Fac. de Ciências e Tecnologia da Universidade de Coimbra, 3030 Coimbra, Portugal
[d]Laboratoire de Métallurgie Physique, Université de Poitiers, 86960 Futuroscope, France

Available online 11 September 2004

Abstract

The main purpose of this work consists on the preparation of single layered zirconium oxynitride, ZrN_xO_y, thin films, deposited by rf reactive magnetron sputtering. The depositions were carried out by varying the process parameters such as substrate bias voltage and flow rate of the reactive gases. Independently of O content, the samples prepared with oxygen fractions revealed crystalline structures basically constituted by face centred cubic ZrN grains. Atomic force microscopy (AFM) observation showed lower values of surface roughness for low oxygen fractions and a second region where roughness grows significantly, corresponding to the highest oxygen fractions. Ion bombardment promoted a continuous smoothing of the surface up to a bias voltage of -66 V. At a bias voltage of -75 V, roughening is again observed. The small increase of film hardness in low oxygen fractions ZrN_xO_y films was attributed to lattice distortions occurring as a result of the possible oxygen incorporation within the ZrN lattice and also grain size reduction. Residual stresses appeared to be an important parameter to explain the observed behaviour, namely in the group of samples prepared with variation in the bias voltage. Regarding colour variations, it was observed a clear dependence of the obtained colorations with oxygen fraction.
© 2004 Elsevier B.V. All rights reserved.

Keywords: ZrN_xO_y; Oxygen fraction; Bias voltage

1. Introduction

Nitrides and oxynitrides represent a group of modern ceramic materials of increasing technological importance. They have been extensively investigated over the past few years because of their remarkable properties in the domains of protective applications, such as wear, diffusion and corrosion-resistant [1–5], but also in opto-electronics and microelectronics [6–8], taking advantage of their property variation possibilities, which result from the change in the concentration of their constituents. Furthermore, their optimum hardness, chemical stability, durability and electronic properties lead to a wide variation of multiple applications that range between the well-known tribological ones [5], such as cutting tools, turbine blades, and other highly abrasive environments, and also those related with optical applications such as solar collectors devices [9,10], just to mention a few.

In modern science, a new field is emerging with increasing application possibilities—the so-called decorative thin films. Decorative hard coatings were first introduced on small consumer products such as watches, writing instruments, eyeglass frames, wristwatches, pens, kitchen and bathroom equipment, as well as jewelry parts. While enhancing the appearance and lending attractive colorations to surfaces, the films are supposed to provide scratch resistance and protection against corrosion and durability. However, the attainable colour tones are largely restricted to some golden yellows, various shades of grey

---

and black tones [11,12], although some attempts have been made to obtain other colours [12].

As a result of technological progress in recent years, a new challenge was passed onto decorative hard coatings. Increasing demands for durability of brass hardware for door locksets and bathroom equipment drive the request for the application of modern PVD processes for these products. In any case, the growing demand for low-cost products and reduced material resources imply that the continuous change in target materials and basic PVD deposition procedures to obtain different coloured films is clearly unsuitable. Taking these restrictions into consideration, recently a new class of materials has been gaining importance for decorative applications, the so-called metal oxynitrides, MeN_xO_y (Me=early transition metal). Their importance results from the presence of oxygen that allows the tailoring of film properties between those of nitride and the correspondent oxides. Tuning the oxide/nitride ratio allows to operators tune the band-gap, bandwidth, and crystallographic order between oxide and nitride and hence the electronic properties of materials and thus their colour.

Despite the huge amount of published scientific works on thin films of metallic nitrides and oxides over the last 20 years [13], the area of metal oxynitrides is poorly explored so far and knowledge of the fundamental mechanism that explains their structural and mechanical behaviour is largely insufficient. To prepare these films, a extremely careful control of the gases flow rates is needed since not only the final properties will depend much on their atomic ratio, but also by the fact that oxygen exhibits a stronger reactivity than nitrogen with regard to the metal [14].

2. Experimental details

ZrN_xO_y samples were deposited by reactive rf magnetron sputtering from a high-purity Zr target onto polished high-speed steel (AISI M2), stainless steel, single crystalline silicon (100) and glass substrates. Substrates were ultra-sonically cleaned and sputter-etched for 15 min in an Ar atmosphere. Depositions were carried out under an Ar/N_2+O_2 atmosphere in an Alcatel SCM650 apparatus, with the substrates rotating at 60 mm over the target at a constant speed of 4 rpm. The base pressure in the deposition chamber was about 10^{-4} Pa and rose to about 4×10^{-1} Pa during depositions. A pure zirconium adhesion layer with a thickness of about 0.30 μm was deposited on each sample to improve adhesion. Films were prepared with variation of the gas flux (N_2+O_2 from 0 to 6.5 sccm), at a constant temperature (573 K) and bias voltages ranging from −75 V up to ground state. Argon flow was kept at 100 sccm.

The chemical composition of the films was determined by Rutherford backscattering spectrometry (RBS), using a 1 MeV $^1H^+$ beam. Ball cratering experiments were used to determine film thickness. The morphology of the films was studied by scanning electron microscopy (SEM) and atomic force microscopy (AFM). The crystallographic structure was investigated by X-ray diffraction in a glancing incidence configuration (GIXRD) with $\theta=2°$ using a monochromatic Cu Kα radiation. Film colour was computed using a commercial CM-2600d portable spectrophotometer from Minolta. Colour specification under the standard CIE illuminant D65 was computed and represented in the CIELAB 1976 colour space [15,16]. The hardness experiments were carried out in a Fischer-scope H100 ultramicrohardness tester, equipped with a Vickers diamond indenter. The applied load was increased in 60 steps (the same for unloading) until the nominal load is reached at 30 mN (maximum load in all tests). The system has a load resolution exceeding 1 μN and the range of the nominal test load is between 4 mN and 1 N. The indentation depths were obtained with an accuracy of 2 nm. Residual stresses, σ_r, were taken from Stoney's equation [17], using substrate curvature radii, both before and after coating deposition [18].

3. Results and discussion

3.1. Deposition rate and chemical composition

RBS composition determination using the RUMP code simulations [19] revealed that although oxygen is extremely reactive in comparison with nitrogen [20], a large range of O contents was possible to be deposited. Homogenous depth composition was obtained in all coatings, as no significant fluctuation was detected in the chemical composition through the thickness of the films. Table 1 presents the composition and thickness of all the samples. The oxygen fraction is determined by the ratio of the oxygen content and the sum of both oxygen and nitrogen contents: $fO_2=C_O/(C_O+C_N)$. These contents were taken from Table 1 and normalized to the zirconium content. The variation of the deposition rate with both oxygen fraction and bias voltage applied to the substrates is plotted in Fig. 1. A systematic decrease in the deposition rate with the increase of the oxygen fraction is revealed. This variation can be explained by taking into account the occurrence of the so-called target poisoning by both reactive gases. A competition phenomenon between removal by sputtering and formation of nitride and oxide layers occurs at the surface of the target. With increasing oxygen fraction (increase in flow rates), the oxide layer formation gains importance over the removal process. Although there is no abrupt transition, one can easily distinguish three different zones corresponding to a high deposition rate for the "pure nitride", an intermediate zone corresponding to the oxynitride films and a low deposition rate corresponding to the highest oxygen fraction (~0.33) and the "pure" oxide. To these zones sequentially corresponds an increase in the oxide layer poisoning of the target—thus making it more difficult for material

Table 1

Thickness and composition of the samples prepared with the same bias voltage (-50 V) and variation of the N/O ratio in the plasma; and variation in the bias voltage at constant N/O ratio in the plasma

Sample	Zr (at.%)	N (at.%)	O (at.%)	V_{bias} (V)	Oxygen fraction	Thickness (μm)
$ZrN_{1.14}O_{0.14}$	44	50	6	-50	0.11	2.3 ± 0.2
$ZrN_{0.91}O_{0.26}$	46	42	12	-50	0.22	3.2 ± 0.1
$ZrN_{0.85}O_{0.28}$	47	40	13	-50	0.25	2.3 ± 0.2
$ZrN_{0.87}O_{0.30}$	46	40	14	-50	0.26	3.0 ± 0.2
$ZrN_{0.87}O_{0.36}$	45	39	16	-50	0.29	3.2 ± 0.2
$ZrN_{0.86}O_{0.41}$	44	38	18	-50	0.32	1.3 ± 0.1
$ZrNO_{0.50}$	40	40	20	-50	0.33	2.0 ± 0.3
$ZrN_{0.81}O_{0.32}$	47	38	15	0	0.28	2.0 ± 0.2
$ZrN_{0.89}O_{0.33}$	45	40	15	-25	0.27	2.5 ± 0.1
$ZrN_{0.80}O_{0.20}$	50	40	10	-66	0.20	1.7 ± 0.2
$ZrN_{0.90}O_{0.10}$	50	45	5	-75	0.10	2.2 ± 0.2

ejection to occur, owing to the lower sputtering rate of the oxide. This behaviour is well correlated with the change of the metalloid concentration (namely that of oxygen). In fact, as oxygen fraction increases, the deposition rate is largely reduced and the sputtering process becomes similar to that observed for the ZrO_2 system. Regarding the variations with the bias voltage, the deposition rate steeply decreases with increasing negative bias voltages in the range 0 to -25 V. The decrease in the deposition rate for negatively biased experiments is a consequence of the improvement in the ion bombardment of the growing films due to the increase in both the bias current, I_s, and the energy of the bombarding ions. Measurement of the bias current showed that I_s rapidly increases for bias voltages in the range from 0 to -50 V, thereafter followed by a smooth increase [21]. The great similarity in the deposition rates throughout the negatively biased samples after this threshold value is the result of this ion current at the substrate, which at -50 V is already as much as that at -66 V and is almost constant for the other negative bias values. Moreover, the increasing ion bombardment promotes film densification, which also contributes to the small decrease in the deposition rate. Ion bombardment reduces not only the deposition rate but also the oxygen fraction in the samples (Table 1). The preferential re-sputtering of oxygen [20], caused by the lower bond strength of the Zr–O with respect to that of Zr–N [22], might be the parameter that can explain this oxygen loss with the increasing bombardment of the growing film.

3.2. Morphology

Cross-sections of the films observed by SEM revealed that the films grow with a columnar-type structure, lying in the transition between T and I zones of Thornton's zone model [23] (Fig. 2a). The process of surface diffusion is not very high (which increases a little with the bias voltage, inducing more compact films) and the films are formed by narrow columnar grains with a densely packed fibrous morphology, with a superficial dome-rounded shape of the

columnar grains [24] as revealed by AFM, Fig. 2b–e). In any case, with the variation of the process parameters, some changes occur as can be observed via AFM results (Fig. 3), where the rms roughness, R_a, calculated from 5×5 μm line scans, is plotted. RMS experimental results were obtained with an accuracy of about 1 nm. In this figure, it is possible to observe two distinct regions corresponding to lower values of surface roughness for low oxygen fractions (including that of ZrN), and a second region where roughness grows significantly, corresponding to the highest oxygen fractions. This increase in roughness, enhancement of the wave profile of the surface, is a consequence of the increase of coating disorder/defects promoted by the possible formation of amorphous oxide phases and the inclusion of oxygen atoms within the grain boundaries or in the ZrN lattice. Furthermore, the variation of roughness suggests a change in the film growth mode from a typical layer by layer in the nitride regime to that of Stranski–Krastanov type mode [20] within the oxynitride regime. This last growth mode is characterized by an island-type film formation, which increases the surface roughness. Regarding the variation of surface roughness with the applied bias, again distinct behaviours can be observed, consisting of a continuous smoothing of the surface up to a bias voltage of -66 V. At a bias voltage of -75 V, a small increase in roughness is observed. Two factors might be competing for this behaviour: first, with increasing bias voltage, there is a reduction of the dome-rounded shape of the surface reduction of the shadowing effect, promoted by the ion bombardment. Such change indicates, as in the former case, a transition from growth regimes. The ion bombardment plays in this case the main role. A high-enough ion flux and subsequently higher surface mobility permits the adatoms to avoid the direct sticking on the top of the columns and diffuse superficially, efficiently filling in
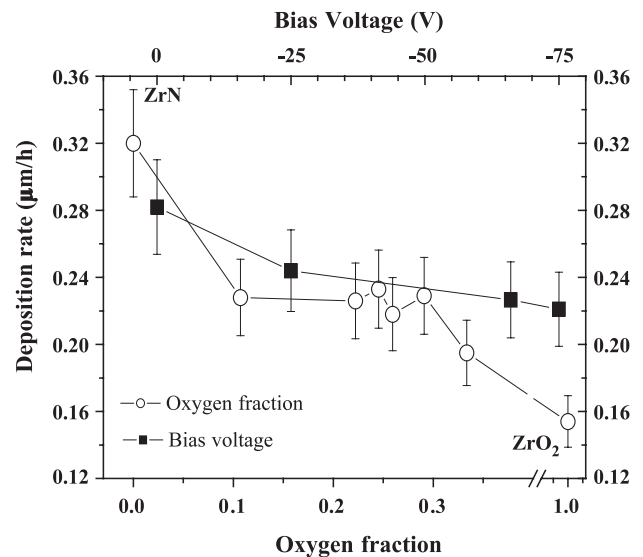

Fig. 1. Variation of the deposition rate of the deposited films as a function of the oxygen fraction and the applied bias voltage to the substrates.
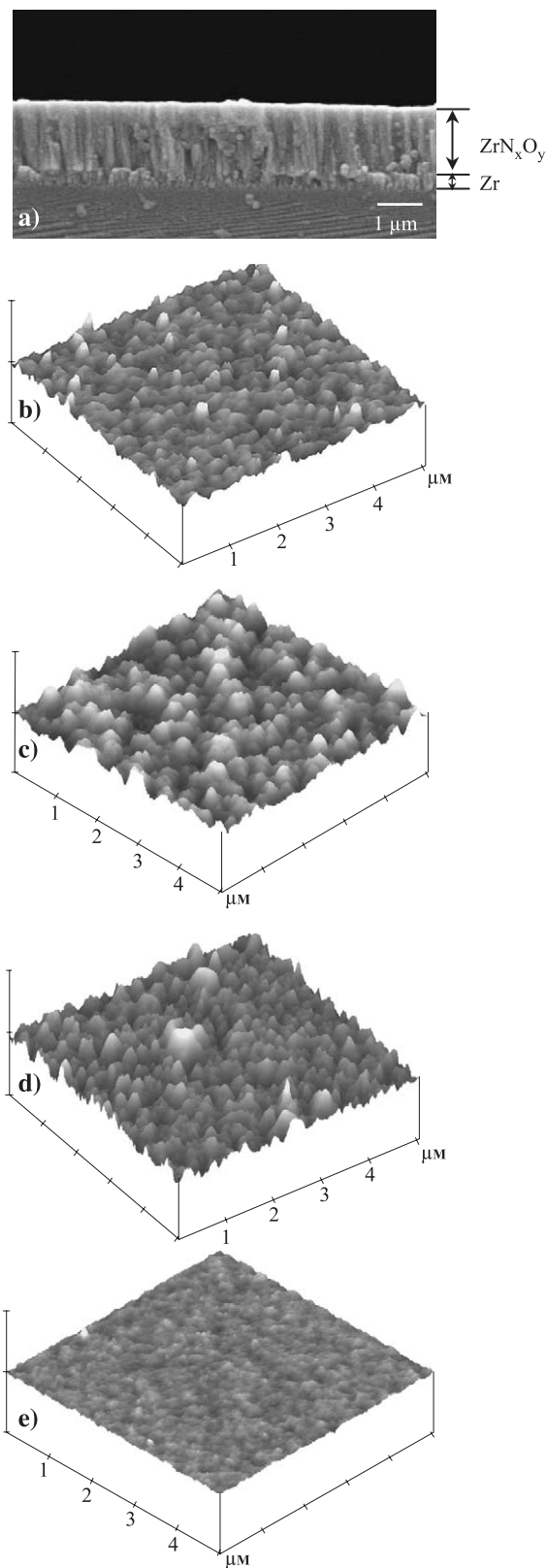
Fig. 2. SEM cross-section of a typical sample from the ZrN_xO_y system (a) and AFM micrographs showing the morphological changes in ZrN_xO_y thin films. The first two micrographs represent changes in samples with different oxygen fractions: (b) $ZrN_{1.14}O_{.14}$ ($fO_2=0.11$) and (c) $ZrN_{.87}O_{.30}$ ($fO_2=0.26$). Micrographs correspond to samples prepared under different bias voltages: (d) no bias applied and (e) −66 V.
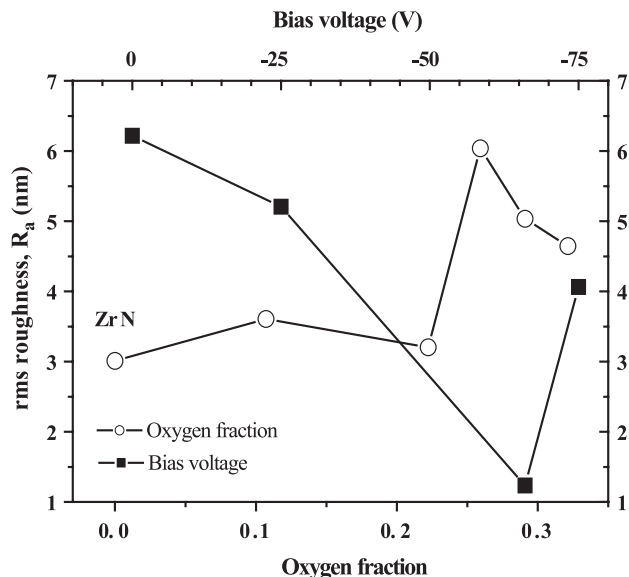

Fig. 3. rms roughness determined from the AFM analysis on a $5×5$ μm area of films prepared with different oxygen fractions and different bias voltages.

more the voids between them. For the highest voltages, ion bombardment becomes too intense and causes an opposite effect, thus increasing the roughness. It has been claimed by some authors that the increase in roughness for higher bias voltages might also be the result of a preferential re-sputtering of an element constituting the film [25].

3.3. Structure

Fig. 4 shows the GIXRD diffraction patterns for the ZrN_xO_y samples. These films exhibit XRD patterns corresponding to an fcc ZrN (space group $Fm-3m$) phase (JCPDS card 65-2905). No diffraction peaks from oxide phases were observed. The diffraction peaks of ZrN phase have slightly different positions for the samples, revealing higher lattice parameters (Fig. 4a(i)) in comparison to the ZrN standard. The changes in the peak position can be related with either the compressive stress or the presence of interstitial oxygen atoms in ZrN lattice. With the increasing amount of oxygen, it is supposed that oxygen could also be in the grain boundaries and/or forming an amorphous oxide phase. In fact, the ZrN grain size seems to decrease with increasing oxygen fraction and the development of a very broad peak around $2\theta=30°$ is an indication of either the amorphization of the ZrN phase induced by the oxygen inclusion or the formation of an amorphous oxide phase.

Regarding the behaviour of samples prepared with increasing bias voltage (Fig. 4b) the main feature that can be observed is a significant change in the peak intensity ratio, $T=I_{(200)}/I_{[(200)+(111)]}$, when going from the unbiased sample to that prepared at −25 V. This fact implies that some kind of texture phenomenon occurs, promoted by the ion bombardment. It is noteworthy that a deeper analysis throughout the entire set of biased samples is made difficult
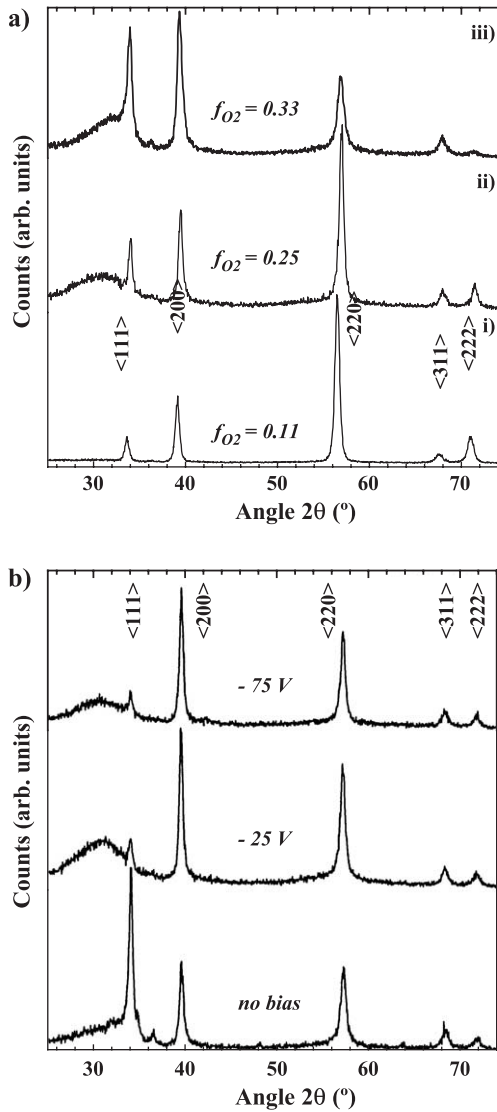
Fig. 4. GIXRD patterns of ZrN$_x$O$_y$ films with different oxygen fractions (a) and prepared at different bias voltages (b).

because, besides the effect of the ion bombardment, composition variation also plays an important role (as noted earlier).

3.4. Hardness and residual stresses

The evolution of hardness as a function of the oxygen fraction is illustrated in Fig. 5. The first conclusion that can be drawn from these results is the good correlation between the different structural changes found and the hardness evolution. For the lower and intermediate oxygen fractions, a small increase in hardness values in comparison to that of "pure" ZrN can be observed. On one hand, it can be attributed to the well-known solid solution hardening mechanism. With oxygen insertion, an increased strength of the material is expected [22] due to lattice distortion. The distortion inhibits the mobility of the dislocations, inducing a hardness enhancement. On the other hand, the other
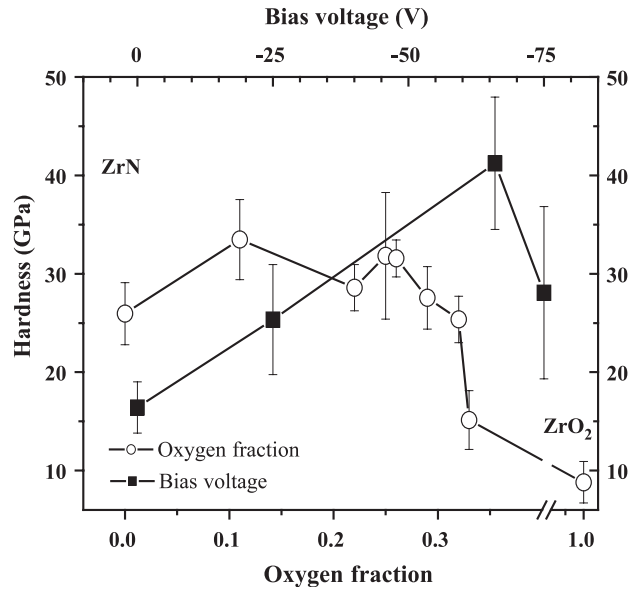

Fig. 5. Hardness of sputtered ZrN$_x$O$_y$ films as a function of the oxygen fraction and the bias voltage.

parameter playing a role in the hardness behaviour is the residual stress state of the samples, as can be particularly indicated by the results shown in Fig. 6, where the residual stress is plotted as a function of the oxygen fraction. In this plot, it is clear that a small increase in oxygen content is followed by an increase in the residual stresses. Further increases in oxygen contents induce a decrease in residual stresses. Generally, samples with the highest compressive stress values are the hardest ones. However, it is clear that this is not the only important parameter for the interpretation of hardness. In fact, for low-stress films (<1.5 GPa), hardness can vary from 15 GPa to more than 30 GPa. The strong increase of the residual stresses with low oxygen contents could be associated with the possible incorporation
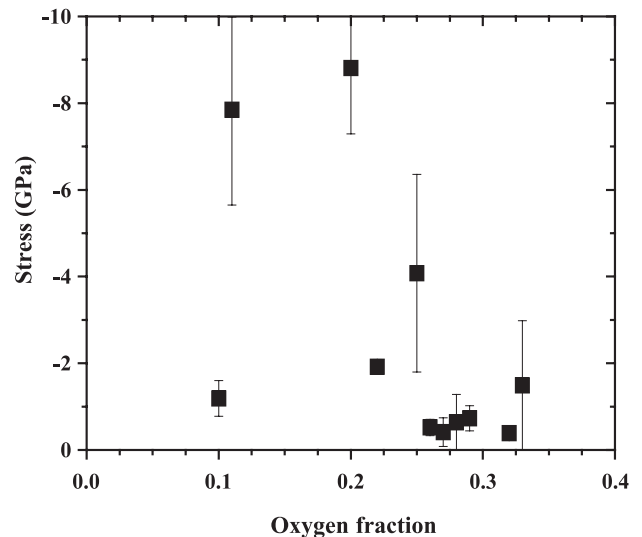

Fig. 6. Residual stresses of sputtered ZrN$_x$O$_y$ films as a function of the oxygen fractions included those prepared with different bias voltages.

of oxygen within the fcc ZrN lattice, which would induce lattice defects in the films structure, acting as obstacles for the dislocation motion [26,27], and thus enhancing hardness.

For the highest oxygen fractions, the trend in hardness is towards the value of the oxide (ZrO_2: prepared in similar conditions than ZrN_xO_y samples). The continuous increase in oxygen fraction would lead to either the amorphization of the ZrN phase or the formation of an amorphous oxide phase, which could explain the hardness reduction.

Concerning stress evolution with substrate bias, an important change in the residual compressive stress from -0.5 to -9 GPa was observed with the increase of the substrate bias, which can be attributed to the ion bombardment, in particular to the well-known atomic peening effect. However, the particular behaviour evidenced by the sample prepared at higher bias voltage (-75 V) and with an oxygen fraction of about 0.1, revealing a residual stress of approximately -1.1 GPa, shows that residual stress is not only bias voltage-dependent but also strongly correlated with the structural features.

3.5. Colour

Fig. 7 shows the average specular colour, represented in the CIELAB 1976 colour space [15,16]. This graph shows that, with increasing oxygen fractions, coatings vary from a bright yellow-pink colour (relatively high positive $b*$ values and relatively low $a*$ values, together with high values of brightness or brilliance, $L*$), which gradually shifts to red-brownish at intermediate oxygen fractions and dark blue for the highest oxygen fractions (negative $b*$ values and relatively low $a*$ values). A significant decrease of the brightness or brilliance, $L*$, of the films with increasing oxygen fraction was also observed, being approximately constant for oxygen fractions higher than ~0.20. These plots suggest a strong dependence of the colour of the films on the oxygen fraction. However, a more detailed analysis of the results might imply that another parameter must play also an important role for colour variation. In fact, samples prepared at -66 V ($ZrN_{.80}O_{.20}$: $fO_2 = {\sim}0.20$) has an oxygen fraction very close to that of $ZrN_{.91}O_{.26}$ ($fO_2 = {\sim}0.22$)
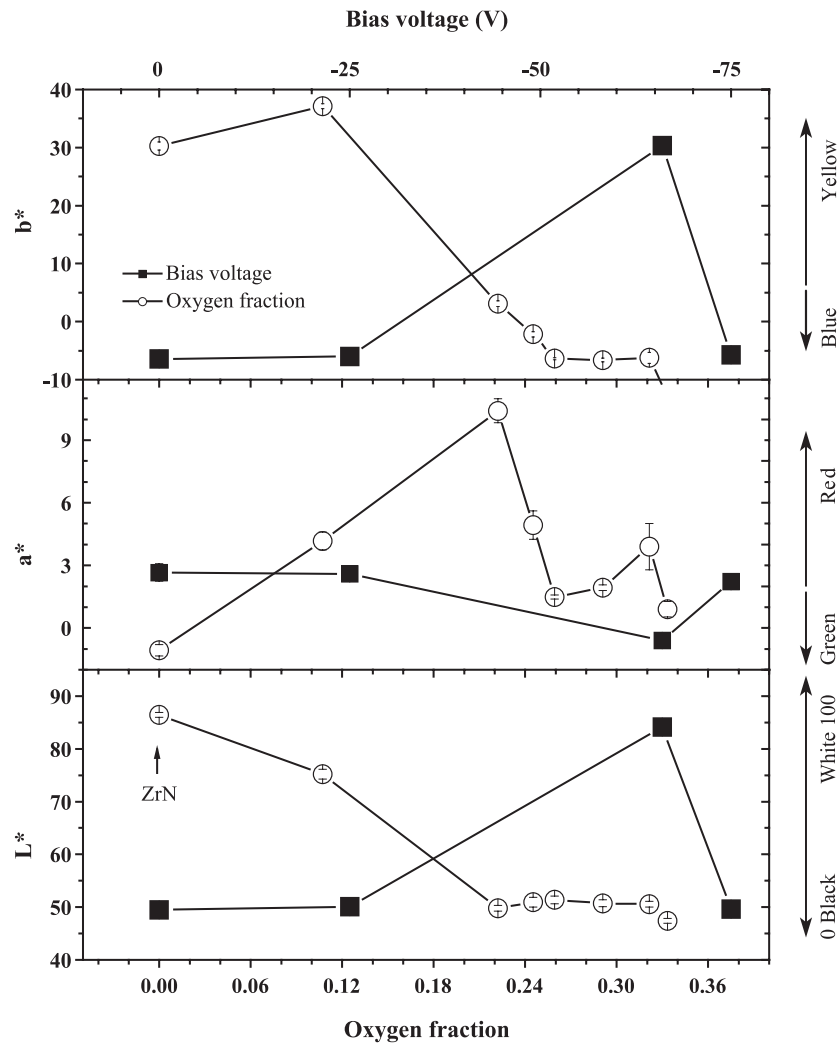

Fig. 7. Average specular colour in the CIELAB 1976 colour space under the standard CIE illuminant D65, for films prepared with different oxygen fractions and different bias voltages.

prepared at -50 V, but very different L^* (~80 in comparison to ~50 for ZrN$_{.91}$O$_{.26}$), a^* (~-0.5 compared to ~10 for ZrN$_{.91}$O$_{.26}$) and b^* (~30 in comparison to ~5 for ZrN$_{.91}$O$_{.26}$). The reason is probably the deficiency in oxygen, as shown by the sample prepared at -66 V. Furthermore, a closer look at Fig. 3 might also be significant for the "singular" behaviour of the -66 V sample. This sample is clearly the one with the lowest surface roughness. This parameter has long been considered to be fundamental in colorimetric features, being one of the main responsible for the variation in the L^* value [12,28]. The different waviness of surface induces differences in the interaction of radiation with film surface and thus differences in coloration, namely that of L^* [12]. A final worthwhile observation is the influence of the residual stresses in colour coordinates. In fact, there is a remarkable difference in the colour coordinates of the sample prepared at -66 V bias, which shows a much higher stress value than the other samples (~-9 GPa; Fig. 6). High compressive stresses are known to affect the microstructure of a material and thus influence all the properties depending on them. Under the influence of externally applied alternating electromagnetic fields, such as light, excitement of bound electrons of a material will occur at higher energy levels. This phenomenon is called selective absorption, and will have a direct effect in the different colours of materials, such as that observed here for that -66 V sample. At any rate, the variation in composition induced by ion bombardment (which also affected the stress levels) will also play an important role for these colour variations.

4. Conclusions

Thin films within the Zr–N–O ternary system were prepared by rf reactive magnetron sputtering. A systematic decrease in the deposition rate with the increase of the oxygen fraction is revealed, which can be explained by the target poisoning by both reactive gases. With the bias voltage, the deposition rate decreases steeply with increasing negative bias voltages in the range 0 to -25 V. Structural characterization results reveal a strong dependence of the film texture on the oxygen fraction. The samples with relatively low fractions of this element revealed only a crystalline structure, which is basically constituted by fcc ZrN grains.

Hardness measurements revealed a small increase with low oxygen fractions, which was attributed to lattice distortions that occurred as a result of oxygen incorporation within the ZrN lattice. Residual stresses were also revealed to be an important factor in the observed behaviour. A small increase in oxygen content is followed by an increase in the residual stresses. Further increases in oxygen contents induce a decrease in residual stresses. Regarding colour

variations, we also observed a clear dependence of the obtained colorations on the oxygen fraction.

Acknowledgements

References

[1] K.H. Jack, Non-Oxide Technical and Engineering Ceramics, Elsevier, Amsterdam, 1986, p. 1.
[2] S. Saito, Fine Ceramics, Elsevier, Tokyo, 1985, p. 197.
[3] S. Komarrneni, J. Mater. Chem. 2 (1992) 1219.
[4] A. Navrotsky, J. Alloys Compd. 321 (2001) 300.
[5] S. Dreer, R. Krismer, P. Wilhartiz, G. Friedbacher, Thin Solid Films 354 (1999) 43.
[6] H. Demiryont, L.R. Thompson, G.J. Collins, J. Appl. Phys. 59 (1986) 3235.
[7] V. Gerova, N.A. Ivanov, K.I. Kirov, Thin Solid Films 81 (1981) 201.
[8] H. Birey, S.-J. Pak, J.R. Sites, J.F. Wager, J. Vac. Sci. Technol. 16 (1979) 2086.
[9] H. Tada, Y. Saito, M. Hitata, M. Hyodo, H. Kawahara, J. Appl. Phys. 73 (1993) 489.
[10] Y. Saito, M. Hirata, H. Tada, M. Hyodo, Appl. Phys. Lett. 63 (1993) 1319.
[11] B. Zega, Surf. Coat. Technol. 39/40 (1989) 507.
[12] C. Mitterer, J. Komenda-Stallmaier, P. Losbichler, P. Schmolz, W.S.M. Werner, H. Stori, Vacuum 46 (1995) 1281.
[13] R. Fraunchy, Surf. Sci. Rep. 38 (2000) 195.
[14] N. Martin, O. Banakh, A.M.E. Santo, S. Springer, R. Sanjinés, J. Takadoum, F. Lévy, Appl. Surf. Sci. 185 (2001) 123.
[15] CIE, Colorimetry, Tech. Rep., 15, Bureau Central de la CIE, 1971, p. 1.
[16] CIE, Recommendations on uniform color spaces, color difference equation and psychometric terms, Tech. Rept. Supplement No. 2 to CIE publication No. 15, Bureau Central de la CIE, 1978, p. 1.
[17] G.G. Stoney, Proc. R. Soc. Lond., A 82 (1909) 172.
[18] For detailed information on the procedure see, F. Vaz, L. Rebouta, P. Goudeau, J.P. Rivière, M. Bodmann, G. Kleer, W. Döll, Thin Solid Films 402 (2002) 195.
[19] L.R. Doolittle, Nucl. Instrum. Methods B9 (1985) 344.
[20] M. Ohring, The Materials Science of Thin Films, Academic Press, San Diego, 1992.
[21] E. Ribeiro, A. Malczyk, S. Carvalho, L. Rebouta, J.V. Fernandes, E. Alves, A.S. Miranda, Surf. Coat. Technol. 151–152 (2002) 515.
[22] D. Sherman, D. Brandon, Handbook of Ceramic Hard Materials, Wiley-VCH, New Jersey, 2000.
[23] J.A. Thornton, Am. Rev. Mater. Sci. 7 (1977) 239.
[24] R. Wuhrer, W. Yeung, M. Phillips, G. McCredie, Thin Solid Films 290–291 (1996) 339.
[25] D. Pilloud, A.S. Dehlinger, J.F. Pierson, A. Roman, L. Pichon, Surf. Coat. Technol. 174–175 (2003) 338.
[26] K. Karlsson, L. Hultman, J.E. Sundgren, Thin Solid Films 371 (2000) 167.
[27] H. Oettel, T. Bertram, V. Weihnacht, R. Wiedemann, S.V. Zitzewitz, Surf. Coat. Technol. 97 (1997) 785.
[28] R. Constantin, B. Miremad, Surf. Coat. Technol. 120–121 (1999) 728.